NORMUON: MAKING MUON MORE EFFICIENT AND SCALABLE

Anonymous authors
Paper under double-blind review

ABSTRACT

The choice of optimizer significantly impacts the training efficiency and computational costs of large language models (LLMs). Recently, the Muon optimizer has demonstrated promising results by orthogonalizing parameter updates, improving optimization geometry through better conditioning. Despite Muon's emergence as a candidate successor to Adam, the potential for jointly leveraging their strengths—has not been systematically explored. In this work, we bridge this gap by proposing NorMuon (Neuron-wise Normalized Muon), an optimizer that synergistically combines orthogonalization with neuron-level adaptive learning rates. Our analysis reveals that while Muon effectively reduces condition numbers, the resulting updates exhibit highly non-uniform neuron norms, causing certain neurons to dominate the optimization process. NorMuon addresses this imbalance by maintaining second-order momentum statistics for each neuron and applying row-wise normalization after orthogonalization, ensuring balanced parameter utilization while preserving Muon's conditioning benefits. To enable practical deployment at scale, we develop an efficient distributed implementation under the FSDP2 framework that strategically distributes orthogonalization computations across devices. Experiments across multiple model scales demonstrate that NorMuon consistently outperforms both Adam and Muon, achieving 21.74% better training efficiency than Adam and 11.31% improvement over Muon on 1.1B pretraining setting, while maintaining a comparable memory footprint to Muon. Our findings suggest that orthogonalization and adaptive learning rates are complementary rather than competing approaches, opening new avenues for optimizer design in large-scale deep learning.

1 INTRODUCTION

Training efficiency remains a central challenge in scaling large language models (LLMs) Sachdeva et al. (2024); Wan et al. (2023), where optimizer choice directly impacts convergence speed, computational requirements, and ultimately, the feasibility of training at scale Jordan et al. (2024b); Wen et al. (2025). The community standard, Adam (Kingma and Ba, 2015), achieves robust performance through coordinate-wise preconditioning: dynamically adjusting learning rates for each parameter based on the second moment of its gradient history. While this per-coordinate adaptivity is computationally efficient and generally stable, it suffers from a fundamental limitation—it treats each parameter independently, ignoring the rich geometric structure and cross-coordinate dependencies inherent in neural network layers.

Recent advances have sought to address this limitation through various approaches to capturing cross-coordinate structure. Adam-mini (Zhang et al., 2025) exploits the near-block-diagonal Hessian structure of neural networks by applying adaptive learning rates to parameter blocks (e.g. each neuron) rather than individual coordinates. More ambitious second-order methods, such as Shampoo (Gupta et al., 2018) and SOAP (Vyas et al., 2024), employ full-matrix preconditioning through singular value decomposition to capture curvature information and parameter interdependencies. However, these approaches incur substantial memory and communication overhead, while introducing hyperparameter sensitivity that limits their practical adoption at scale.

Recently, Muon (Jordan et al., 2024b) has emerged as a compelling middle ground, applying truncated Newton-Schulz iterations to approximate the orthogonal polar factor of momentum matrices.

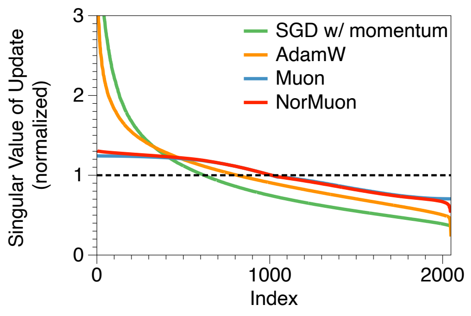

(a) Singular value distribution of update directions

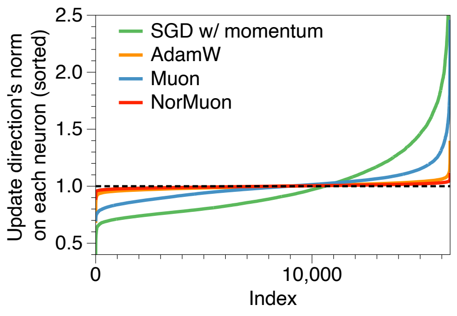

(b) Per-neuron update norm

Figure 1: Analysis of optimization geometry during 1.1B model pretraining. We examine the up-projection matrix in the 8th layer's MLP at the middle checkpoint. (a) Singular value distribution reveals that raw momentum and AdamW's update exhibit high condition numbers. Muon's orthogonalization effectively eliminates this imbalance. (b) Despite Muon's improved conditioning, the L^2 norm of individual neuron updates still shows high variance. AdamW achieves much more uniform per-neuron norms. Our proposed NorMuon maintains Muon's low condition number while normalizing neuron contributions.

This approach yields matrix-wise orthogonalized updates that improve conditioning while maintaining modest computational overhead and approximately half the memory consumption of Adam, demonstrating promising results in LLM training.

These optimizers fundamentally differ in their preconditioning granularity and objectives. Adam and Adam-mini, when considered without exponential moving averages (EMAs), apply L^2 normalization at the per-coordinate and per-neuron levels respectively, adjusting learning rates while preserving update signs. In contrast, the idealized version of Shampoo and Muon operate at the per-matrix level, actively orthogonalizing parameter updates.

The varied preconditioning strategies employed by these optimizers raise an important question: *Are different forms of preconditioning inherently conflicting, or can they be combined in a way that yields complementary benefits?*

To investigate this, we analyzed key properties of the update matrices from different optimizers during pretraining of a 1.1B-parameter Transformer model, examining both singular value distributions and per-neuron norms. As illustrated in Figure 1a, raw momentum accumulates updates with extremely high condition numbers, indicating that certain directions dominate while leaving other parameters underutilized. AdamW produces moderately more balanced singular values, though the improvement remains limited. In contrast, Muon's approximate orthogonalization successfully addresses this conditioning issue, yielding well-balanced singular values across the spectrum. However, examining per-neuron update norms (Figure 1b) reveals a complementary perspective. AdamW demonstrates superior performance in reducing variance across per-neuron update norms compared to SGD momentum. Conversely, while Muon's orthogonalization effectively improves matrix-level conditioning, the per-neuron update norms exhibit high variance, with some neurons receiving disproportionately large updates relative to others.

This observation motivates our key insight: while Muon's orthogonalization effectively reduces the condition number of updates, the remaining high variance in neuron norms still creates an imbalanced learning dynamic, potentially leading to inefficient parameter usage. Drawing inspiration from Adam-mini's success Zhang et al. (2025) with per-neuron adaptive learning rates, we propose to incorporate second-order momentum to normalize these disparate scales and ensure more balanced parameter updates. Our method, **NorMuon**, augments Muon's orthogonalization with neuron-wise adaptive learning rates computed from accumulated second-order statistics. As demonstrated in our analysis, NorMuon yields updates with both low condition numbers (Figure 1a) and uniform neuron norms (Figure 1b), thereby combining the advantages of Muon and AdamW and achieving more balanced utilization of the network's representational capacity.

Beyond algorithmic innovation, the distributed implementation of orthogonalization-based optimizers remains relatively underexplored in the literature. To enable training at larger scales, we develop a distributed version of NorMuon compatible with the FSDP2 framework (Feng et al., 2022). While previous work on distributed Muon (Liu et al., 2025a) was implemented using ZeRO-1 with Megatron-LM (Rajbhandari et al., 2020; Shoeybi et al., 2019), FSDP2 can offer greater flexibility and memory efficiency. However, direct adaptation of the previous distributed approach to FSDP2 would result in extensive replicated computation, as FSDP2 shards nearly all parameters across devices. Our implementation addresses this challenge by distributing orthogonalization computation across devices, eliminating redundant calculations while maintaining load balance. Furthermore, we leverage FSDP2's row-wise parameter sharding to enable efficient neuron-wise normalization without incurring additional communication overhead.

In summary, our contributions are threefold:

• We propose NorMuon, a simple and effective optimizer that combines Muon's orthogonalization with neuron-wise adaptive learning rates. NorMuon maintains uniform neuron norms to ensure balanced parameter utilization while preserving the low condition number achieved by Muon's orthogonalization.

• We develop an efficient distributed implementation under the FSDP2 framework. By carefully orchestrating sharded optimizer states, we gather updated momentum and distribute Muon orthogonalization computation uniformly across GPUs, achieving optimal memory efficiency with manageable communication and computational overhead.

• Through extensive experiments across multiple scales of LLM pretraining, we demonstrate that orthogonalization and blockwise adaptive learning rates are complementary rather than conflicting, with their combination yielding superior training dynamics compared to either approach in isolation.

2 Related Works and Background

2.1 Related Works

Adaptive Gradient Methods. The introduction of per-parameter adaptive learning rates has been instrumental in training deep networks. Optimizers such as AdaGrad (Duchi et al., 2011), RMSProp (Hinton, 2012), Adam (Kingma and Ba, 2015) and AdamW (Loshchilov and Hutter, 2017) use first- and second-moment estimates to adjust each weight's step size individually. This coordinate-wise preconditioning improves stability and convergence in heterogeneous settings, and has become the de facto standard for LLM training. However, treating each weight independently ignores the underlying structure of neural network layers and incurs high memory overhead by storing two extra tensors per parameter. This memory cost motivated techniques like AdaFactor (Shazeer and Stern, 2018), which factorizes the second-moment accumulator across rows and columns to reduce memory. Similarly, Adam-mini (Zhang et al., 2025) partitions parameters into blocks (e.g. each neuron's weights) and assigns a single learning rate to each block, matching AdamW's performance on different model sizes, while halving memory cost. GaLore (Zhao et al., 2024) maintains momentum in a low-rank subspace derived from the SVD of gradients, although its effectiveness diminishes for long sequence lengths (Liu et al., 2025b). Lion (Chen et al., 2023) applies a coordinate-wise signed update, abandoning second-order moment estimates to achieve memory savings.

Second-order Methods. In parallel, other optimizers capture the rich geometry of the loss surface by coupling updates across parameters. K-FAC (Martens and Grosse, 2015) and its variants (Martens et al., 2018; Gao et al., 2021) approximate curvature information beyond individual coordinates, capturing correlations across parameters. Shampoo (Gupta et al., 2018) and its distributed variant (Shi et al., 2023) employ Kronecker-factored preconditioners and have demonstrated strong performance in practice (Dahl et al., 2023). More recently, SOAP (Vyas et al., 2024) establishes a connection between Shampoo and Adafactor and further improves convergence performance. Despite these advances, Shampoo and SOAP incur substantial memory cost and computational overhead, which hinders their applicability at LLM scale.

Orthogonal Update Methods: Muon (Momentum Orthogonalized by Newton-Schulz, Jordan et al. (2024b)) represents a breakthrough that leverages matrix geometry without the full cost of second-order methods. Muon performs an approximate polar decomposition (via Newton–Schulz iterations) on the momentum to extract its orthogonal component and also eliminates the need to store second-order momentum. Muon thus simultaneously improves both convergence and memory efficiency compared to Adam, demonstrating great potential for scaling up model pretraining (Liu et al., 2025a; Shah et al., 2025). We provide a detailed description of the Muon algorithm in Section 2.2. More recently, Dion (Ahn et al., 2025) extends the orthogonal update paradigm to be more communication- and compute-efficient in distributed settings. Dion applies a low-rank orthonormalization scheme via amortized power iteration instead of full Newton–Schulz, and decouples momentum buffers across devices to avoid full gradient synchronization.

2.2 Background: Muon optimizer

Muon (Jordan et al., 2024b) is an optimizer designed for the 2D weight matrices in neural network hidden layers. The key innovation lies in orthogonalizing the momentum before applying parameter updates, thereby improving the conditioning of the optimization trajectory. Formally, at iteration t, given weight matrix W_{t-1}, learning rate η_t, and loss function L, Muon maintains a first-order momentum M_t and computes updates as:

$$M_t = \mu\, M_{t-1} + \nabla L(W_{t-1}), \tag{1}$$
$$O_t = \mathrm{NS5}(M_t), \tag{2}$$
$$W_t = W_{t-1} - \eta_t\, O_t, \tag{3}$$

where $M_0 = \mathbf{0}$ and μ is the momentum coefficient. The critical component is the orthogonalization operator $\mathrm{NS5}(\cdot)$, which aims to approximate the orthogonal projection of the momentum matrix:

$$\mathrm{Ortho}(M) = \arg\min_O \{\|O - M\|_F : O^\top O = I \text{ or } OO^\top = I\}. \tag{4}$$

Muon approximates this orthogonalization through a fixed number of Newton-Schulz iterations. Starting with the Frobenius-normalized momentum $X_0 = M_t / \|M_t\|_F$, the algorithm performs N iterations (typically $N = 5$):

$$X_k = a\, X_{k-1} + b\,(X_{k-1}X_{k-1}^\top)\, X_{k-1} + c\,(X_{k-1}X_{k-1}^\top)^2\, X_{k-1}, \quad k = 1, \dots, N, \tag{5}$$

with the final orthogonalized update $O_t = X_N$. The coefficients (a, b, c) are carefully chosen such that singular values of the update matrix converge toward unity. In practice, Muon is typically applied only to 2D weight matrices in hidden layers, while scalar parameters, bias vectors, embeddings, and unembedding layers continue to use standard optimizers such as Adam.

3 Method

In this section, we introduce NorMuon, where we aim to combine Muon's orthogonalization with block-wise adaptive learning rates based on the observation that the approximated orthogonalized updates can experience a high variance on update directions norm of each neuron.

Algorithm 1 NorMuon

```
1:  Input: Initial weights $\mathbf{W}_0 \in \mathbb{R}^{m\times n}$, loss $L$, learning rate $\eta$, momentum parameters $(\beta_1, \beta_2)$,
    perturbation parameter $\varepsilon$, weight decay $\lambda$.
2:  Initialize $\mathbf{M}_0 \in \mathbb{R}^{m\times n} \leftarrow \mathbf{0}$, $\mathbf{v}_0 \in \mathbb{R}^{m} \leftarrow \mathbf{0}$
3:  for $t = 1, 2, \dots$ do
4:      $\mathbf{G}_t \leftarrow \nabla_{\mathbf{W}} L(\mathbf{W}_t)$
5:      $\mathbf{M}_t \leftarrow \beta_1 \mathbf{M}_{t-1} + (1-\beta_1)\mathbf{G}_t$
6:      $\mathbf{O}_t \leftarrow \mathrm{NS5}(\mathbf{M}_t)$
7:      $\mathbf{v}_t \leftarrow \beta_2 \mathbf{v}_{t-1} + (1-\beta_2)\,\mathrm{mean}_{\mathrm{cols}}(\mathbf{O}_t \odot \mathbf{O}_t)$
8:      $\mathbf{V}_t \leftarrow \mathrm{ExpandRows}(\mathbf{v}_t)$                    $(\mathbf{V}_t \in \mathbb{R}^{m\times n})$
9:      $\widehat{\mathbf{O}}_t \leftarrow \mathbf{O}_t \oslash \left(\sqrt{\mathbf{V}}_t + \varepsilon\right)$
10:     $\hat{\eta} = 0.2\eta\sqrt{mn}/||\widehat{\mathbf{O}}_t||_F$
11:     $\mathbf{W}_{t+1} \leftarrow \mathbf{W}_t - \eta\lambda\mathbf{W}_t - \hat{\eta}\widehat{\mathbf{O}}_t$
12: end for
```

3.1 NorMuon

We present our update rule in Algorithm 1. The algorithm maintains two momentum states: the standard first-order momentum $\mathbf{M}_t \in \mathbb{R}^{m \times n}$ used by Muon (line 5), and an averaged second-order momentum $\mathbf{v}_t \in \mathbb{R}^m$ that tracks the squared magnitude of each neuron's update direction (lines 7). Importantly, $\mathbf{v}_t$ requires minimal additional memory overhead, storing only m scalars compared to the $m \times n$ first-order momentum.

At each iteration and given the gradient, we first follow the Muon's update rule that update the first-order momentum and apply Newton-Schulz iteration for orthogonalization (line 4-6), producing $\mathbf{O}_t$ with improved conditioning. Rather than directly using this orthogonalized update, we compute row-wise statistics to capture the per-neuron update magnitudes. Specifically, we calculate the mean squared value across columns for each row of $\mathbf{O}_t$ (line 7). This statistic is accumulated into our averaged second-order momentum $\mathbf{v}_t$ using exponential moving average with decay rate β_2. We then apply $\mathbf{v}_t$ for row-wise normalization (line 9). This second-order momentum is similar to Adam-mini's (Zhang et al., 2025) block-wise reduced-dimensional statistics, where we treat each neuron (i.e. each row) as a block. As illustrated in Figure 1, this normalization reduces the variance in update magnitudes across neurons while preserving the favorable conditioning properties.

We observe that after the row-normalization the resulting update matrix has a much larger norm. Hence, during the update, we add a learning rate scaling following Jordan et al. (2024b) to keep a similar RMS norm to match Adam's RMS norm (line 10). The constant 0.2 is adopted from prior work as an empirically tuned stability factor; it effectively controls the post-normalization step size and can be further adjusted. Moreover, because this scaling already regulates the RMS norm, we omit the bias-correction commonly used in Adam-style methods, as the correction would be neutralized by the scaling.

We would like to note that in the idealized case where the $\mathbf{O}_t$ is strictly orthogonalized (i.e., not approximated by NS5), the per-neuron norm would be strictly 1 for full-rank matrix with $m \leq n$. On these matrices, the neuron-wise normalization would not be beneficial. However, since orthogonalization is approximated in practice, we observe that this normalization remains necessary and helpful even for $m \leq n$ matrix (validated in Section 4.1.4).

3.2 Distributed NorMuon

As LLM training scales larger, distributed training becomes essential for both memory constraints and computational efficiency. We develop a distributed version of NorMuon compatible with the FSDP2 framework (Feng et al., 2022), which employs ZeRO-3 style (Rajbhandari et al., 2020) sharding to partition optimizer states, parameters, and gradients across multiple devices.

While coordinate-wise optimizers like Adam naturally extend to distributed settings, NorMuon presents unique challenges due to Muon's orthogonalization step, which requires access to complete momentum matrices. An existing distributed implementation of Muon (Liu et al., 2025a) gathers the full momentum on all devices and replicates the orthogonalization computation. We avoid such replicated costs by near-uniformly assign parameters to different devices.

Algorithm 2 presents our distributed implementation. The key modifications from Algorithm 1 are:

• **Efficient Orthogonalization Distribution** (line 5-9): Rather than having all devices compute orthogonalization for all parameters, we first sort the parameter list by matrix size (line 2) to ensure uniform work assignment, where Numel$(\cdot)$ counts the number of elements in each matrix. We then assign each parameter tensor to a specific device using a round-robin scheme. Only the assigned device gathers the full momentum matrix via all-gather communication and performs the Newton-Schulz orthogonalization (lines 5-8), before scattering the result back to all devices (line 9). This approach eliminates redundant computation while maintaining load balance across devices.

• **Shard-Local Row Normalization** (lines 10-12): An advantage of our design is that the row-wise normalization operates entirely on local shards without additional communication. This is possible because FSDP2 employs row-wise sharding, ensuring that each device holds complete rows of the weight matrix. The computation of row statistics and normalization thus proceed independently.

Importantly, while row-wise sharding aligns naturally with NorMuon, the algorithm is not restricted to this setting. NorMuon can also operate under more complex sharding schemes—e.g. tensor parallelism or column-wise sharding—by aggregating per-row statistics through a lightweight all-reduce before applying the same normalization. The communication overhead relative to Muon remains negligible, since it involves only per-row scalar reductions (<1% of the parameter size). Designing optimal distributed variants of Muon itself under these more intricate sharding configurations is an interesting avenue for future work, and we believe our formulation provides a practical building block for scaling orthogonalization-based optimizers to larger clusters.

Algorithm 2 Distributed NorMuon: one iteration

```
1: **Input:** Sharded 2D weights $\{\mathbf{W}^{(i)}_{\text{shard}}\}_{i=0,\ldots,N}$, Sharded gradient $\{\mathbf{G}^{(i)}_{\text{shard}}\}_{i=0,\ldots,N}$, learning rate $\eta$, momentum parameters $(\beta_1, \beta_2)$, perturbation parameter $\varepsilon$, weight decay $\lambda$. We omit the initialization of optimizer states for simplicity.
2: $\{\mathbf{W}^{(i)}_{\text{shard}}\}_{i=0,\ldots,N} \leftarrow \text{Sort}(\{\mathbf{W}^{(i)}_{\text{shard}}\}_{i=0,\ldots,N}, \text{key} = \text{Numel}(\cdot))$
3: for $i = 0, 1, \ldots, N$ do
4:     $\mathbf{M}^{(i)}_{\text{shard}} \leftarrow \beta_1 \mathbf{M}^{(i)}_{\text{shard}} + (1 - \beta_1)\mathbf{G}^{(i)}_{\text{shard}}$
5:     if $i$ mod world size == current rank then
6:         $\mathbf{M}^{(i)} \leftarrow \text{Gather}(\mathbf{M}^{(i)}_{\text{shard}})$
7:         $\mathbf{O}^{(i)} \leftarrow \text{NS5}(\mathbf{M}^{(i)})$
8:     end if
9:     $\mathbf{O}^{(i)}_{\text{shard}} \leftarrow \text{Scatter}(\mathbf{O}^{(i)})$
10:    $\mathbf{v}^{(i)}_{\text{shard}} \leftarrow \beta_2 \mathbf{v}^{(i)}_{\text{shard}} + (1 - \beta_2)\, \text{mean}_{\text{cols}}(\mathbf{O}^{(i)}_{\text{shard}} \odot \mathbf{O}^{(i)}_{\text{shard}})$
11:    $\mathbf{V}^{(i)}_{\text{shard}} \leftarrow \text{ExpandRows}\left(\mathbf{v}^{(i)}_{\text{shard}}\right)$
12:    $\widehat{\mathbf{O}}^{(i)}_{\text{shard}} \leftarrow \mathbf{O}^{(i)}_{\text{shard}} \oslash \left(\sqrt{\mathbf{V}^{(i)}_{\text{shard}}} + \varepsilon\right)$
13:    $\hat{\eta} = 0.2\eta\sqrt{\text{Numel}(\widehat{\mathbf{O}}^{(i)}_{\text{shard}})}/||\widehat{\mathbf{O}}^{(i)}_{\text{shard}}||_F$
14:    $\mathbf{W}^{(i)}_{\text{shard}} \leftarrow \mathbf{W}^{(i)}_{\text{shard}} - \eta\lambda \mathbf{W}^{(i)}_{\text{shard}} - \hat{\eta}\widehat{\mathbf{O}}^{(i)}_{\text{shard}}$
15: end for
```

3.3 Overhead Analysis

Memory Overhead. NorMuon maintains Muon's memory efficiency. For a weight matrix $W \in \mathbb{R}^{m\times n}$, the memory consumption of optimizer states for each optimizer is: (1) Adam: $2mn$ (first and second-order momentum); (2) Muon: mn (first-order momentum only); (3) NorMuon: $m(n + 1)$ (first-order momentum + per-neuron second-order statistics). The additional memory overhead of NorMuon compared to Muon is negligible (1/n factor), while remaining approximately 50% more memory-efficient than Adam.

Communication Overhead. NorMuon introduces moderate additional communication compared to standard FSDP training. Under FP32 training with AdamW, the per-parameter communication cost is: 4 bytes (forward all-gather) + 4 bytes (backward all-gather) + 4 bytes (gradient reduce-scatter) = 12 bytes. With NS5 iteration computed in BF16 precision, NorMuon requires: 12 bytes (standard FSDP communication) + 2 bytes (momentum gather, BF16) + 2 bytes (update scatter, BF16) = 16 bytes.

This represents a 33% increase in communication volume. When parameters use BF16, the relative overhead increases to 50%. However, this communication can be overlapped with orthogonalization computation to minimize latency impact. More specifically, we group parameters and (i) launch an asynchronous gather for group 1; (ii) once group 1 is ready, launch the gather for group 2 while performing orthogonalization on group 1; (iii) iterate this process over all groups. We see communication overlap as an implementation optimization and hence ommit the details in Algorithm 2 for simplicity. Please refer to Appendix D for an illustration of the pipeline. In our experiments (Section 4.1.5), we demonstrate that the per-iteration latency of NorMuon is only 3% higher than AdamW, while achieving significantly better convergence efficiency.

4 Experiments

In this section, we conduct pretraining experiments across four different model scales to validate the effectiveness of NorMuon: 124M, 350M, 1.1B, and 5.4B parameters. For the larger models (1.1B and 5.4B), we adopt the experimental setup from previous work on architecture scaling (Ren et al., 2025), with results and configurations presented in Section 4.1. For the smaller models (124M and 350M), we follow the experimental setting of Modded-NanoGPT (Jordan et al., 2024a), with results and settings provided in Section 4.2. We include extensive ablation studies that justify our design choices, along with detailed efficiency analyses (Section 4.1.4 and 4.1.5).

4.1 Experiments on 1.1B and 5.4B Models

4.1.1 Setup

Models. We follow a simple linear rule from prior works (Kaplan et al., 2020; Ren et al., 2025) for scaling the architectural shape. Specifically, for a model with depth d layers, we configure the architecture as follows: hidden dimension αd, number of attention query heads d, number of attention key-value heads $d/4$, and MLP intermediate dimension $4\alpha d$, where $\alpha = 128$. The α and ratios are derived relative to Llama-3-8B (Dubey et al., 2024). Our 1.1B and 5.4B parameter models correspond to depths of $d = 16$ and $d = 28$ layers, respectively.

Dataset. We conduct pretraining on the SlimPajama dataset (Soboleva et al., 2023). The 1.1B and 5.4B models are trained on 50B and 100B tokens, respectively—corresponding to approximately $2\times$ and $1\times$ the Chinchilla token budget. Additional results for the 1.1B model trained at the $1\times$ Chinchilla setting (20B tokens) are provided in Appendix A.2.

Hyperparameters. We first tune the hyperparameters on the 1.1B model as base, then we employ Depth-μp (Yang et al., 2023) to scale the learning rate inversely proportional to $\sqrt{d}$ based on model depth. The base learning rate is set to 4×10^{-4} with a base model depth of 16. The learning rate schedule consists of a 1B token warmup phase followed by linear decay to 0. We apply 0.1 weight decay for 2D parameters in hidden layers and zero weight decay for others to enhance training stability (Ren et al., 2025). The batch size is fixed at 2M tokens with a sequence length of 4096 tokens. For optimization, we use the following configurations: Adam optimizer with $(\beta_1, \beta_2) = (0.9, 0.95)$, Muon optimizer with $\beta_1 = 0.95$ following Jordan et al. (2024b), and our proposed NorMuon optimizer with $(\beta_1, \beta_2) = (0.95, 0.95)$. More details on the hyperparameters tuning are provided in Appendix A.1

Baselines. We compare NorMuon against three established optimizers: AdamW (Loshchilov and Hutter, 2017), the standard adaptive optimizer with decoupled weight decay; Muon (Jordan et al., 2024b), which applies orthogonalization to update directions; and Dion (Ahn et al., 2025), a scalable orthogonalization-based method that uses low-rank power iteration. For all orthogonalization-based optimizers (including NorMuon), we apply orthogonalization to the 2D weight matrices in the hidden layers, covering attention projections (QKV and output projections) and MLP up/down projections. Following standard practice (Jordan et al., 2024b), embeddings, layer norms, biases, and the LM head are trained with AdamW. We concatenate the QKV matrices along the output dimension prior to orthogonalization, as we found no performance benefits from separating them.

4.1.2 Main results

Figure 2 presents the validation loss curve across different model scales. NorMuon demonstrates consistent and substantial improvements over all baseline optimizers. While orthogonalization-based optimizers (Muon and Dion) already outperform AdamW, NorMuon amplifies this advantage through the integration of our proposed neuron-wise adaptive learning rate.

To quantify the performance gains, Table 1 reports the percentage reduction in training steps required for each optimizer to achieve the same final validation loss as Adam. NorMuon achieves the best efficiency gains of 21.74% and 13.17% for the 1.1B and 5.4B models, respectively.

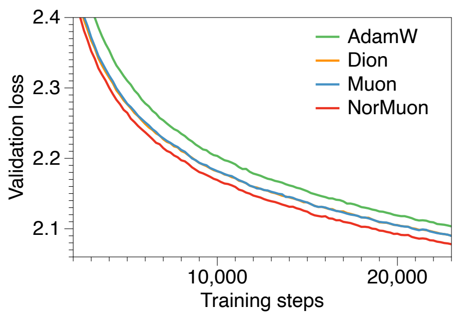

(a) Pretraining results of 1.1B model.

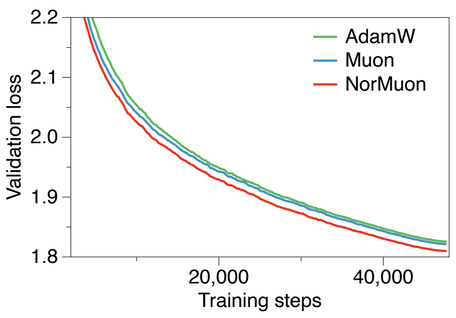

(b) Pretraining results of 5.4B model.

Figure 2: Comparison of different optimizers on pretraining on 1.1B (a) and 5.4B (b) Transformers. NorMuon outperforms other baselines by notable margin.

Table 1: Efficiency Gain over Adam. Calculated as percentage reduction in training steps required to reach the same final loss achieved by Adam. Dion's performance on 5.4B model is excluded due to resource constraints and similar performance with Muon on 1.1B scale.

Optimizer	**1.1B Model (%)**	**5.4B Model (%)**
Muon	10.43	5.60
Dion	10.43	–
NorMuon	21.74	13.17

4.1.3 Benchmark performance.

We further evaluate the 1.1B and 5.4B pretrained models using standard pretraining tasks, including OpenBookQA (Mihaylov et al., 2018), HellaSwag (Zellers et al., 2019), ARC-Easy (Clark et al., 2018), WSC273 (Levesque et al., 2012), Winogrande (Sakaguchi et al., 2020), BoolQ (Clark et al., 2019), and PIQA (Bisk et al., 2020) As shown in Table 2, across both model sizes, NorMuon achieves the best average downstream performance and yields the best results on almost all tasks.

Table 2: Downstream benchmark performance of 1.1B and 5.4B pretrained models.

Model	Optimizer	**Avg.**	OpenBookQA	HellaSwag	ARC-E	WSC273	Winogrande	BoolQ	PIQA
1.1B	AdamW	53.80	31.00	47.35	53.45	62.64	53.12	59.14	69.91
	Muon	53.91	31.60	48.12	55.22	58.24	52.57	**60.76**	70.89
	NorMuon	**55.34**	**33.40**	**48.70**	**55.85**	**65.57**	**53.43**	59.51	**70.95**
5.4B	AdamW	60.59	35.60	59.98	62.79	**72.16**	58.48	61.62	73.50
	Muon	60.65	35.40	59.99	63.51	72.10	58.33	60.73	**74.48**
	NorMuon	**61.74**	**36.40**	**61.35**	**63.93**	**72.16**	**60.30**	**63.46**	74.59

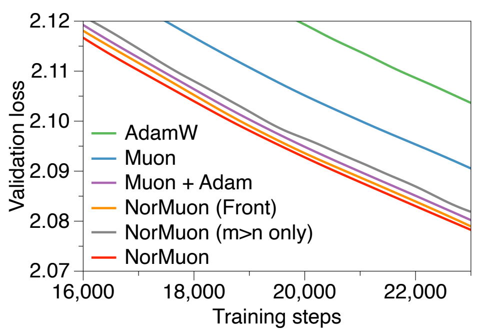

Figure 3: Ablation studies of NorMuon on 1.1B pretraining experiments.

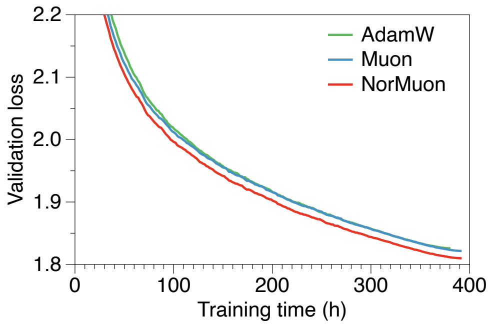

Figure 4: Validation loss vs wallclock time on 5.4B pretraining experiments.

4.1.4 Ablation studies.

To validate our design choices in NorMuon, we conduct ablation studies that examine three key aspects: the granularity of adaptive learning rates and the positioning of normalization relative to orthogonalization, and the impact of applying normalization universally versus selectively based on matrix dimensions. The results on pretraining 1.1B model are presented in Figure 3.

Adaptive Learning Rate Granularity. We compare our neuron-wise adaptive approach against coordinate-wise adaptation in the "Muon+Adam" baseline, which applies Adam's coordinate-wise normalization after Muon's orthogonalization. This approach is similarly explored in concurrent work (Si et al., 2025), though we removed the sign stabilization component as we found it performs better without it. While Muon+Adam demonstrates improvements over vanilla Muon, it underperforms NorMuon across the training trajectory. Importantly, this approach requires maintaining full second-order momentum of orthogonalized updates, doubling the memory overhead (Section 4.1.5).

Normalization Positioning. We further investigate whether the positioning of adaptive normalization matters by testing "NorMuon (Front)", which applies neuron-wise adaptive learning rates before orthogonalization rather than after. This variant still improves upon Muon, but slightly underperforms NorMuon.

Universal vs. Selective Normalization: To test whether normalization is beneficial to $m \leq n$ matrices as discussed in Section 3.1, we evaluate "NorMuon ($m > n$ only)", which applies normalization only to $m > n$ matrices. We can see that this selective approach underperforms the full NorMuon, demonstrating that applying normalization to those with $m \leq n$ is helpful.

4.1.5 Computational and Memory Overhead Analysis

In this section, we demonstrate that the overheads incur by NorMuon are manageable and do not diminish the practical benefits.

Wall-Clock Performance. Figure 4 presents the validation loss as a function of wall-clock training time. Despite the additional computation required for orthogonalization and neuron-wise normalization, NorMuon maintains substantial performance advantages over AdamW.

Memory and Computational Overhead. Table 3 provides a breakdown of the computational and memory requirements for each optimizer. NorMuon achieves comparable memory efficiency to Muon with nearly a 50% reduction compared to AdamW or Muon + Adam. In terms of computational cost, NorMuon introduces only a 2.9% increase in training step time compared to AdamW. We can observe that forward and backward passes dominate the training step time, making the cost of optimizer step relatively small. NorMuon's neuron-wise norm computation adds minimal cost relative to orthogonalization operations. Table 3 is profiled on 16 GPUs setting, we also include results on 32 GPUs in Appendix A.6.

We further profile the step time of NorMuon under two ablated configurations: (i) without communication overlap and (ii) without our orthogonalization distribution strategy. As shown in Table 3, communication overlap provides a clear reduction in optimizer-step latency, while distributing the orthogonalization workload across GPUs is critical for keeping overhead low. Removing this distribution increases the optimizer-step time by approximately 2.7×. Importantly, this distributed orthogonalization strategy can be and has been applied to Muon as well, ensuring a fair comparison between the two methods.

4.2 Experiments on Modded-NanoGPT

To further verify the advantages of NorMuon over Muon, we conduct experiments using Muon's original experimental setting on Modded-NanoGPT (Jordan et al., 2024a).

Models. The model architecture is consistent with GPT-2 (Radford et al., 2019), with 124M and 350M parameter configurations obtained by adjusting width and depth.

Dataset. We train all models on the FineWeb dataset (Penedo et al., 2024). The 124M model is trained on approximately 3.2B tokens, while the 350M model uses approximately 4B tokens. We also include results on C4 dataset (Raffel et al., 2020) in Appendix A.3.

Table 3: Computational and memory overhead comparison for different optimizers when training a 5.4B parameter model. Training step time includes forward pass, backward pass, and optimizer step. Percentages indicate relative increase compared to AdamW baseline.

Optimizer	Memory cost of optimizer states (GB)	Optimizer step time (s)	Training step time (s)
AdamW	40.56	0.02	28.73
Muon	21.14	0.83	29.56 (2.8%↑)
Muon + Adam	40.56	0.85	29.58 (3.0%↑)
NorMuon	21.19	0.84	29.57 (2.9%↑)
w/o communication overlap	-	1.31	30.04 (4.5%↑)
w/o orthogonalization distribution	-	2.29	31.04 (8.1%↑)

Hyperparameters. Since Muon has already performed extensive hyperparameter tuning in this setting (Jordan et al., 2024b), we adopt their optimized configurations except for β_1, which we slightly tune. We use a batch size of 512, sequence length of 1024, and the Warmup-Stable-Decay (WSD) learning rate schedule. Training iterations are set to 6,200 for the 124M model and 7,500 for the 350M model. Keeping the default hyperparameters, we use the same learning rate for NorMuon, and conduct a grid search over $\beta_1 \in \{0.9, 0.95\}$, reporting the best result. We set β_2 in NorMuon to 0.95.

Results. Figure 5 presents the comparison between NorMuon and Muon on 124M and 350M parameter models. NorMuon consistently outperforms Muon across both model sizes. Since Muon's improvements over Adam have been extensively demonstrated in Jordan et al. (2024b), we omit those baseline comparisons here.

To quantify the computational benefits of NorMuon, we conduct an additional analysis where Muon is trained with the same learning rate schedule but for a longer total number of iterations, until it reaches the same validation loss as NorMuon (denoted as "Muon-rescale" in Figure 5). We observe that on the 124M model, Muon requires 6% more iterations than NorMuon to achieve the same validation loss. On the 350M model, this efficiency gap increases substantially to 15%, demonstrating the broad advantage of NorMuon over Muon.

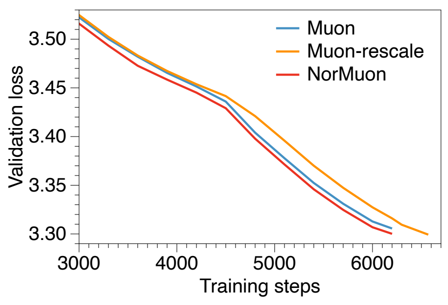

(a) Pretraining results of 124M model.

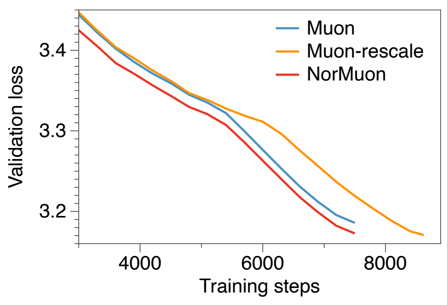

(b) Pretraining results of 350M model.

Figure 5: Comparison of Muon and NorMuon on pretraining 124M (a) and 350M (b) Modded-NanoGPT on FineWeb. NorMuon outperforms Muon by notable margin.

5 CONCLUSION

In this work, we introduced **NorMuon**, a simple yet effective optimizer that integrates Muon's orthogonalization with neuron-wise adaptive learning rates. To make NorMuon practical for large-scale training, we developed an efficient distributed implementation under the FSDP2 framework, carefully orchestrating momentum gathering and orthogonalization to eliminate redundant computation and communication overhead. Our experiment results shows notable improvement over Muon, demonstrating that orthogonalization and adaptive scaling need not be mutually exclusive, but can be complementary, when combined, lead to superior optimization dynamics.

References

Ahn, K., Xu, B., Abreu, N. and Langford, J. (2025). Dion: Distributed orthonormalized updates. *arXiv preprint arXiv:2504.05295*.

Bisk, Y., Zellers, R., Bras, R. L., Gao, J. and Choi, Y. (2020). PIQA: reasoning about physical commonsense in natural language. In *AAAI*. AAAI Press.

Chen, X., Liang, C., Huang, D., Real, E., Wang, K., Pham, H., Dong, X., Luong, T., Hsieh, C.-J., Lu, Y. et al. (2023). Symbolic discovery of optimization algorithms. *Advances in neural information processing systems*, **36** 49205–49233.

Clark, C., Lee, K., Chang, M., Kwiatkowski, T., Collins, M. and Toutanova, K. (2019). Boolq: Exploring the surprising difficulty of natural yes/no questions. In *NAACL-HLT (1)*. Association for Computational Linguistics.

Clark, P., Cowhey, I., Etzioni, O., Khot, T., Sabharwal, A., Schoenick, C. and Tafjord, O. (2018). Think you have solved question answering? try arc, the AI2 reasoning challenge. *CoRR*, **abs/1803.05457**.

Dahl, G. E., Schneider, F., Nado, Z., Agarwal, N., Sastry, C. S., Hennig, P., Medapati, S., Eschenhagen, R., Kasimbeg, P., Suo, D. et al. (2023). Benchmarking neural network training algorithms. *arXiv preprint arXiv:2306.07179*.

Dubey, A., Jauhri, A., Pandey, A., Kadian, A., Al-Dahle, A., Letman, A., Mathur, A., Schelten, A., Yang, A., Fan, A. et al. (2024). The llama 3 herd of models. *arXiv e-prints* arXiv–2407.

Duchi, J., Hazan, E. and Singer, Y. (2011). Adaptive subgradient methods for online learning and stochastic optimization. *Journal of machine learning research*, **12**.

Face, H. (2025). Open r1: A fully open reproduction of deepseek-r1. `https://github.com/huggingface/open-r1`

Feng, W., Constable, W. and Mao, Y. (2022). Getting started with fully sharded data parallel (fsdp2). `https://docs.pytorch.org/tutorials/intermediate/FSDP_tutorial.html`.

Gao, K., Liu, X., Huang, Z., Wang, M., Wang, Z., Xu, D. and Yu, F. (2021). A trace-restricted kronecker-factored approximation to natural gradient. In *Proceedings of the AAAI Conference on Artificial Intelligence*, vol. 35.

Gupta, V., Koren, T. and Singer, Y. (2018). Shampoo: Preconditioned stochastic tensor optimization. In *International Conference on Machine Learning*. PMLR.

Hinton, G. (2012). rmsprop: Divide the gradient by a running average of its recent magnitude. `https://www.cs.toronto.edu/~tijmen/csc321/slides/lecture_slides_lec6.pdf`

Jordan, K., Bernstein, J., Rappazzo, B., @fernbear.bsky.social, Vlado, B., Jiacheng, Y., Cesista, F., Koszarsky, B. and @Grad62304977 (2024a). modded-nanogpt: Speedrunning the nanogpt baseline. `https://github.com/KellerJordan/modded-nanogpt`

Jordan, K., Jin, Y., Boza, V., You, J., Cesista, F., Newhouse, L. and Bernstein, J. (2024b). Muon: An optimizer for hidden layers in neural networks. `https://kellerjordan.github.io/posts/muon/`

Kaplan, J., McCandlish, S., Henighan, T., Brown, T. B., Chess, B., Child, R., Gray, S., Radford, A., Wu, J. and Amodei, D. (2020). Scaling laws for neural language models. *arXiv preprint arXiv:2001.08361*.

Kingma, D. P. and Ba, J. (2015). Adam: A method for stochastic optimization. In *3rd International Conference on Learning Representations, ICLR 2015, San Diego, CA, USA, May 7-9, 2015, Conference Track Proceedings* (Y. Bengio and Y. LeCun, eds.).
http://arxiv.org/abs/1412.6980

Levesque, H. J., Davis, E. and Morgenstern, L. (2012). The winograd schema challenge. *KR*, **2012** 3.

Lightman, H., Kosaraju, V., Burda, Y., Edwards, H., Baker, B., Lee, T., Leike, J., Schulman, J., Sutskever, I. and Cobbe, K. (2023). Let's verify step by step. *arXiv preprint arXiv:2305.20050*.

Liu, J., Su, J., Yao, X., Jiang, Z., Lai, G., Du, Y., Qin, Y., Xu, W., Lu, E., Yan, J. et al. (2025a). Muon is scalable for llm training. *arXiv preprint arXiv:2502.16982*.

Liu, L., Xu, Z., Zhang, Z., Kang, H., Li, Z., Liang, C., Chen, W. and Zhao, T. (2025b). Cosmos: A hybrid adaptive optimizer for memory-efficient training of llms. *arXiv preprint arXiv:2502.17410*.

Loshchilov, I. and Hutter, F. (2017). Decoupled weight decay regularization. *arXiv preprint arXiv:1711.05101*.

Martens, J., Ba, J. and Johnson, M. (2018). Kronecker-factored curvature approximations for recurrent neural networks. In *International Conference on Learning Representations*.

Martens, J. and Grosse, R. (2015). Optimizing neural networks with kronecker-factored approximate curvature. In *International conference on machine learning*. PMLR.

Mihaylov, T., Clark, P., Khot, T. and Sabharwal, A. (2018). Can a suit of armor conduct electricity? A new dataset for open book question answering. In *EMNLP*. Association for Computational Linguistics.

Penedo, G., Kydlíček, H., allal, L. B., Lozhkov, A., Mitchell, M., Raffel, C., Werra, L. V. and Wolf, T. (2024). The fineweb datasets: Decanting the web for the finest text data at scale. In *The Thirty-eight Conference on Neural Information Processing Systems Datasets and Benchmarks Track*.
https://openreview.net/forum?id=n6SCkn2QaG

Radford, A., Wu, J., Child, R., Luan, D., Amodei, D., Sutskever, I. et al. (2019). Language models are unsupervised multitask learners. *OpenAI blog*, **1** 9.

Raffel, C., Shazeer, N., Roberts, A., Lee, K., Narang, S., Matena, M., Zhou, Y., Li, W. and Liu, P. J. (2020). Exploring the limits of transfer learning with a unified text-to-text transformer. *Journal of machine learning research*, **21** 1–67.

Rajbhandari, S., Rasley, J., Ruwase, O. and He, Y. (2020). Zero: Memory optimizations toward training trillion parameter models. In *SC20: International Conference for High Performance Computing, Networking, Storage and Analysis*. IEEE.

Rein, D., Hou, B. L., Stickland, A. C., Petty, J., Pang, R. Y., Dirani, J., Michael, J. and Bowman, S. R. (2024). GPQA: A graduate-level google-proof q&a benchmark. In *First Conference on Language Modeling*.
https://openreview.net/forum?id=Ti67584b98

Ren, L., Chen, C., Xu, H., Kim, Y. J., Atkinson, A., Zhan, Z., Sun, J., Peng, B., Liu, L., Wang, S. et al. (2025). Decoder-hybrid-decoder architecture for efficient reasoning with long generation. *arXiv preprint arXiv:2507.06607*.

Sachdeva, N., Coleman, B., Kang, W.-C., Ni, J., Hong, L., Chi, E. H., Caverlee, J., McAuley, J. and Cheng, D. Z. (2024). How to train data-efficient llms. *arXiv preprint arXiv:2402.09668*.

Sakaguchi, K., Bras, R. L., Bhagavatula, C. and Choi, Y. (2020). Winogrande: An adversarial winograd schema challenge at scale. In *AAAI*. AAAI Press.

Shah, I., Polloreno, A. M., Stratos, K., Monk, P., Chaluvaraju, A., Hojel, A., Ma, A., Thomas, A., Tanwer, A., Shah, D. J. et al. (2025). Practical efficiency of muon for pretraining. *arXiv preprint arXiv:2505.02222*.

Shazeer, N. and Stern, M. (2018). Adafactor: Adaptive learning rates with sublinear memory cost. In *International Conference on Machine Learning*. PMLR.

Shi, H.-J. M., Lee, T.-H., Iwasaki, S., Gallego-Posada, J., Li, Z., Rangadurai, K., Mudigere, D. and Rabbat, M. (2023). A distributed data-parallel pytorch implementation of the distributed shampoo optimizer for training neural networks at-scale. *arXiv preprint arXiv:2309.06497*.

Shoeybi, M., Patwary, M., Puri, R., LeGresley, P., Casper, J. and Catanzaro, B. (2019). Megatron-lm: Training multi-billion parameter language models using model parallelism. *arXiv preprint arXiv:1909.08053*.

Si, C., Zhang, D. and Shen, W. (2025). Adamuon: Adaptive muon optimizer. *arXiv preprint arXiv:2507.11005*.

Soboleva, D., Al-Khateeb, F., Myers, R., Steeves, J. R., Hestness, J. and Dey, N. (2023). SlimPajama: A 627B token cleaned and deduplicated version of RedPajama. `https://www.cerebras.net/blog/slimpajama-a-627b-token-cleaned-and-deduplicated-version-of-redpajama`. `https://huggingface.co/datasets/cerebras/SlimPajama-627B`

Vyas, N., Morwani, D., Zhao, R., Kwun, M., Shapira, I., Brandfonbrener, D., Janson, L. and Kakade, S. (2024). Soap: Improving and stabilizing shampoo using adam. *arXiv preprint arXiv:2409.11321*.

Wan, Z., Wang, X., Liu, C., Alam, S., Zheng, Y., Liu, J., Qu, Z., Yan, S., Zhu, Y., Zhang, Q. et al. (2023). Efficient large language models: A survey. *arXiv preprint arXiv:2312.03863*.

Wen, K., Hall, D., Ma, T. and Liang, P. (2025). Fantastic pretraining optimizers and where to find them. *arXiv preprint arXiv:2509.02046*.

Yang, A., Zhang, B., Hui, B., Gao, B., Yu, B., Li, C., Liu, D., Tu, J., Zhou, J., Lin, J. et al. (2024). Qwen2. 5-math technical report: Toward mathematical expert model via self-improvement. *arXiv preprint arXiv:2409.12122*.

Yang, G., Yu, D., Zhu, C. and Hayou, S. (2023). Tensor programs vi: Feature learning in infinite-depth neural networks. *arXiv preprint arXiv:2310.02244*.

Zellers, R., Holtzman, A., Bisk, Y., Farhadi, A. and Choi, Y. (2019). Hellaswag: Can a machine really finish your sentence? In *ACL (1)*. Association for Computational Linguistics.

Zhang, P., Zeng, G., Wang, T. and Lu, W. (2024). Tinyllama: An open-source small language model.

Zhang, Y., Chen, C., Li, Z., Ding, T., Wu, C., Kingma, D. P., Ye, Y., Luo, Z. and Sun, R. (2025). Adam-mini: Use fewer learning rates to gain more. In *The Thirteenth International Conference on Learning Representations, ICLR 2025, Singapore, April 24-28, 2025*. OpenReview.net.
`https://openreview.net/forum?id=iBExhaU3Lc`

Zhao, J., Zhang, Z., Chen, B., Wang, Z., Anandkumar, A. and Tian, Y. (2024). Galore: Memory-efficient llm training by gradient low-rank projection. *arXiv preprint arXiv:2403.03507*.

A Additional Experiments

A.1 Hyperparameters tuning of main experiments.

In this subsection, we describe how the base hyperparameters were selected for the main experiments and the additional tuning performed to evaluate robustness.

For the 1.1B model, we directly adopt the hyperparameters from TinyLlama (Zhang et al., 2024) for the AdamW baseline, as these settings are already well-tuned. To further verify this, we conduct an additional hyperparameter sweep under the 1× Chinchilla token budget, and the results (shown below) confirm that the adopted configuration is near-optimal.
For the Muon baseline, we tune only the learning rate while keeping all other hyperparameters fixed, except for β_1, which we set to 0.95 following the original Muon blog. For NorMuon, to avoid any implicit tuning bias, we use exactly the same hyperparameters as Muon and vary only the learning-rate ratio.

To ensure a rigorous comparison across optimizers, we perform a controlled hyperparameter sweep on the 1.1B model trained with a 1× Chinchilla budget (20B tokens). For each optimizer, we sweep over: learning rate (for AdamW) or learning-rate ratio (for Muon/NorMuon), EMA coefficients β_1, β_2, and weight decay. For Muon and NorMuon, we tune the learning-rate ratio (Algorithm 1)—not the raw learning rate—consistent with prior work (Liu et al., 2025a). The results are summarized below; the top two configurations for each optimizer are bolded. The first row in each block corresponds to the configuration used in the main experiments.

Table 4: Hyperparameters Sweep of AdamW

Learning Rate	β_1	β_2	WD	Val. Loss
4e-4	0.9	0.95	0.1	**2.176**
2e-4	–	–	–	2.242
8e-4	–	–	–	2.182
–	0.8	–	–	2.203
–	0.95	–	–	2.179
–	–	0.9	–	2.176
–	–	0.98	–	2.190
–	–	–	0	2.213
–	–	–	0.2	**2.174**

Table 5: Hyperparameters Sweep of Muon

Learning Rate Ratio	β_1	WD	Val. Loss
0.2	0.95	0.1	**2.134**
0.1	–	–	2.154
0.4	–	–	**2.135**
–	0.9	–	2.175
–	0.98	–	2.145
–	–	0	2.189
–	–	0.2	2.144

Across all sweeps, additional tuning yields minimal improvements, confirming that the current configurations were already well-chosen. Importantly, the best NorMuon configuration consistently achieves lower validation loss than the best Muon and AdamW settings, further supporting its robustness.

Table 6: Hyperparameters Sweep of NorMuon

Learning Rate Ratio	β_1	β_2	WD	Val. Loss
0.2	0.95	0.95	0.1	**2.128**
0.1	–	–	–	2.144
0.4	–	–	–	**2.128**
–	0.9	–	–	2.167
–	0.98	–	–	2.135
–	–	0.9	–	2.128
–	–	0.98	–	2.134
–	–	–	0	2.176
–	–	–	0.2	2.134

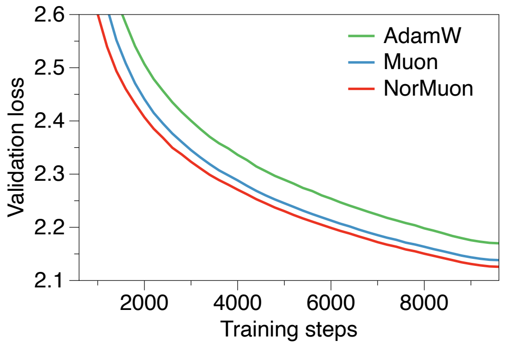

Figure 6: Pretraining results of 1.1B model on 20B tokens.

A.2 Experiments of 1.1B model trained on 20B tokens.

Figure 6 presents the validation loss curve 1.1B model trained on 20B tokens. NorMuon demonstrates consistent improvements. NorMuon achieves the best efficiency gains of 25.04%, outperforming Muon by 5.88%.

A.3 Experiments on Modded-NanoGPT with C4 dataset

The original Modded-NanoGPT leaderboard adopt the FineWeb dataset. To further demonstrate the robustness and generality of NorMuon, we replicate the benchmark using a different large-scale corpus, the C4 dataset (Raffel et al., 2020). Following the 1×Chinchilla token budget, we train a 124M model on approximately 3B tokens and a 350M model on 7B tokens, and we re-tune the hyperparameters of both Muon and NorMuon for this new setting.

As shown in Figure 7, NorMuon consistently achieves lower validation loss than Muon across the entire training trajectory for both model sizes. When we extend Muon's training long enough to match NorMuon's final validation loss, Muon requires approximately 6% more optimization steps. These findings mirror the trends observed on FineWeb, further supporting that NorMuon provides more sample-efficient training across datasets and scales.

A.4 Ablation Experiments on Modded-NanoGPT

To further verify the effectiveness of NorMuon, we conducted several ablation experiments under the setting of training a 350M Modded-NanoGPT on FineWeb, and show the results in Figure 8:

(1) Standard NorMuon, denoted as "NorMuon" in Figure 8.

(2) Standard Muon used in original setting of Modded-NanoGPT (Jordan et al., 2024b), denoted as "Muon" in Figure 8.

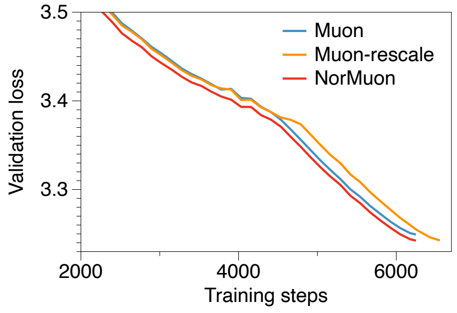

(a) Pretraining results of 124M model.

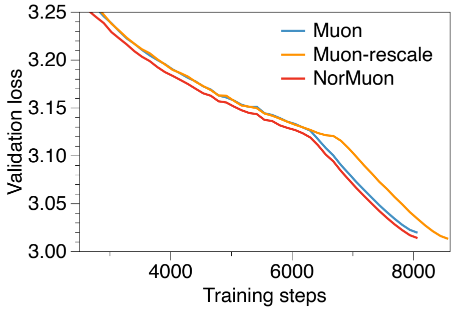

(b) Pretraining results of 350M model.

Figure 7: Comparison of Muon and NorMuon on pretraining 124M (a) and 350M (b) Modded-NanoGPT on C4. NorMuon shows consistently lower validation loss throughout training.

(3) Applying normalization directly to Muon's update such that the update is strictly $\sqrt{m \times n}$, denoted as "Muon w/ normalization" in Figure 8.

(4) applying NorMuon only to weight matrices with $m > n$, while using the normalized muon mentioned in (3) for all other weight matrices, denoted as "NorMuon ablation" in Figure 8.

We can see that although Muon with normalization performs slightly better than Muon in the early stages, it is eventually surpassed by Muon, indicating that the effectiveness of NorMuon cannot be attributed to normalization. Furthermore, since weight matrices with $m > n$ correspond only to the MLP up-projection matrices, which constitute only a small portion of the model, applying NorMuon only to this subset of parameters greatly diminishes the effect of NorMuon, resulting in only a marginal improvement over Muon.

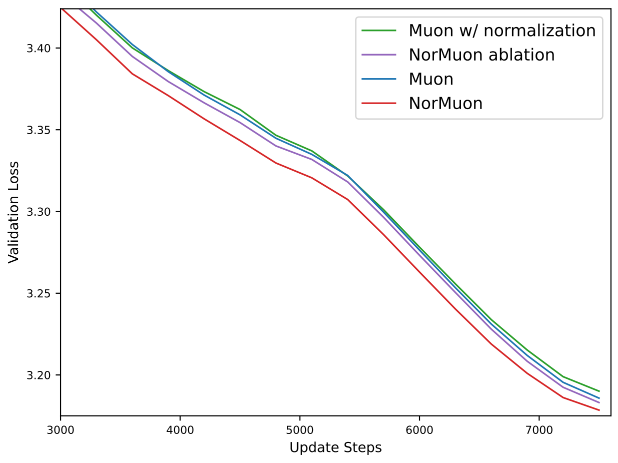

Figure 8: Ablation studies on pretraining 350M model.

A.5 Supervised Finetuning Experiments.

To further validate the effectiveness of NorMuon beyond pretraining, we additionally evaluate it in a supervised fine-tuning (SFT) setting. We perform long-reasoning mathematical SFT using Qwen 2.5 Math 7B (Yang et al., 2024) as the base model. The model is fine-tuned on the Mixture-of-Thoughts (Face, 2025) dataset, where we use a subset of 87k prompts covering mathematics and science. Following prior work, we assess downstream performance on MATH 500 (Lightman et al., 2023), AIME 2024, AIME 2025, and GPQA Rein et al. (2024).

As shown in Table 7, NorMuon attains the highest average score and achieves the best performance on most individual tasks. These results demonstrate that NorMuon remains effective in the SFT

Optimizer	Avg	MATH 500	AIME24	AIME25	GPQA
AdamW	43.36	80.60	25.73	23.96	43.18
Muon	43.58	81.20	**27.50**	23.49	42.11
NorMuon	**44.02**	**82.20**	26.60	**24.69**	**42.61**

Table 7: Supervised fine-tuning evaluation on mathematical reasoning benchmarks.

Table 8: Overhead on 32 GPUs. NorMuon adds only 2.9% overhead in total step time.

Model	**Optimizer Step Time (s)**	**Training Step Time (s)**
Adam	0.016	14.99
NorMuon	0.460	15.43 (+2.9%)

regime, not just in pretraining. We also note that prior work (Liu et al., 2025a) highlights that the alignment between pretraining and fine-tuning optimizers can notably influence downstream performance. Therefore, the benefits of NorMuon may be even more pronounced when applied to LLMs that were pretrained with Muon-like optimizers.

A.6 Step time with 32 A100 GPUs.

On a 32-GPU configuration, we measure the per-step optimizer time and end-to-end training step time for both Adam and NorMuon. The results are summarized in Table 8. As shown, NorMuon incurs only a 2.9% overhead in total training step time relative to Adam, despite a larger per-optimizer computation. This minimal slowdown arises from two factors: (i) the forward and backward passes dominate overall wall-clock time; and (ii) as GPU count increases, our distributed orthogonalization scheme parallelizes across devices, reducing per-GPU optimizer cost.

B Implementation Details

For experiments involving 1.1B and 5.4B parameter models, we conducted training on 2 nodes, each equipped with 8 A100 GPUs (80GB) connected via NVLink for optimized inter-GPU communication. Training duration was approximately 2 days for the 1.1B model and 7 days for the 5.4B model.

All experiments using Modded-NanoGPT, including both 124M and 350M parameter models, were performed on a single node with 8 A100 GPUs.

C Experiment Setup of Modded-NanoGPT

We strictly follow the experimental setup of Muon (Jordan et al., 2024b), with details below:

Models: The model architecture is consistent with GPT-2 (Radford et al., 2019), with 124M and 350M parameter configurations obtained by adjusting width and depth.

Dataset: We train all models on the FineWeb dataset (Penedo et al., 2024). The 124M model is trained on approximately 3.2B tokens, while the 350M model uses approximately 4B tokens.

Hyperparameters: Since Muon has already performed extensive hyperparameter tuning in this setting (Jordan et al., 2024b), we adopt their optimized configurations except for β_1, which we slightly tune. We use a batch size of 512, sequence length of 1024, and the Warmup-Stable-Decay (WSD) learning rate schedule. Training iterations are set to 6,200 for the 124M model and 7,500 for the 350M model.

For the 124M model, Adam's parameters uses a learning rate of 3.6×10^{-3} with momentum parameters $(\beta_1, \beta_2) = (0.9, 0.95)$. For Muon and NorMuon, we set the learning rate to 3.6×10^{-4} and conduct a grid search over $\beta_1 \in \{0.9, 0.95\}$, reporting the best result. For NorMuon, β_2 is set to 0.95.

For the 350M model, Adam employs differentiated learning rates: 0.3 for the embedding layer and 3×10^{-3} for the output layer, with momentum parameters $(\beta_1, \beta_2) = (0.8, 0.95)$. For hidden layers, Muon and NorMuon use a learning rate of 7.5×10^{-4}, with β_1 selected from $\{0.9, 0.95\}$ based on validation performance.

D Communication Overlap Timeline Visualization

To aid understanding of our distributed optimizer design, we provide a timeline visualization (Fig. 9) illustrating the inter-group pipelining used in NorMuon. For clarity, we depict a simplified example with three parameter groups and two GPUs. This figure represents the idealized scheduling pattern; in practice, the exact boundaries of the communication and computation blocks may vary depending on parameter sizes, communication bandwidth, and hardware characteristics.

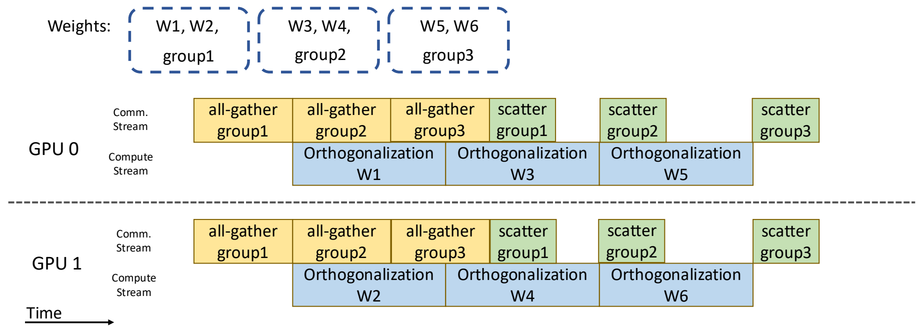

Figure 9: Timeline visualization of the distributed NorMuon optimizer, showing how all-gather for group $k+1$ overlaps with orthogonalization of group k across separate CUDA streams.

E Visualization of Updates' singular value and neuron norm.

Figure 10, figure 11, and figure 12 present the visualization of updates' singular value and neuron norms similar to figure 1 on different training stages and layers.

F LLM Usage

In preparing this paper, large language models (LLMs) such as ChatGPT were used only for light editing purposes, including minor grammar checking and sentence polishing. No part of the research ideation, methodology design, experimental execution, or analysis was conducted with the assistance of LLMs.

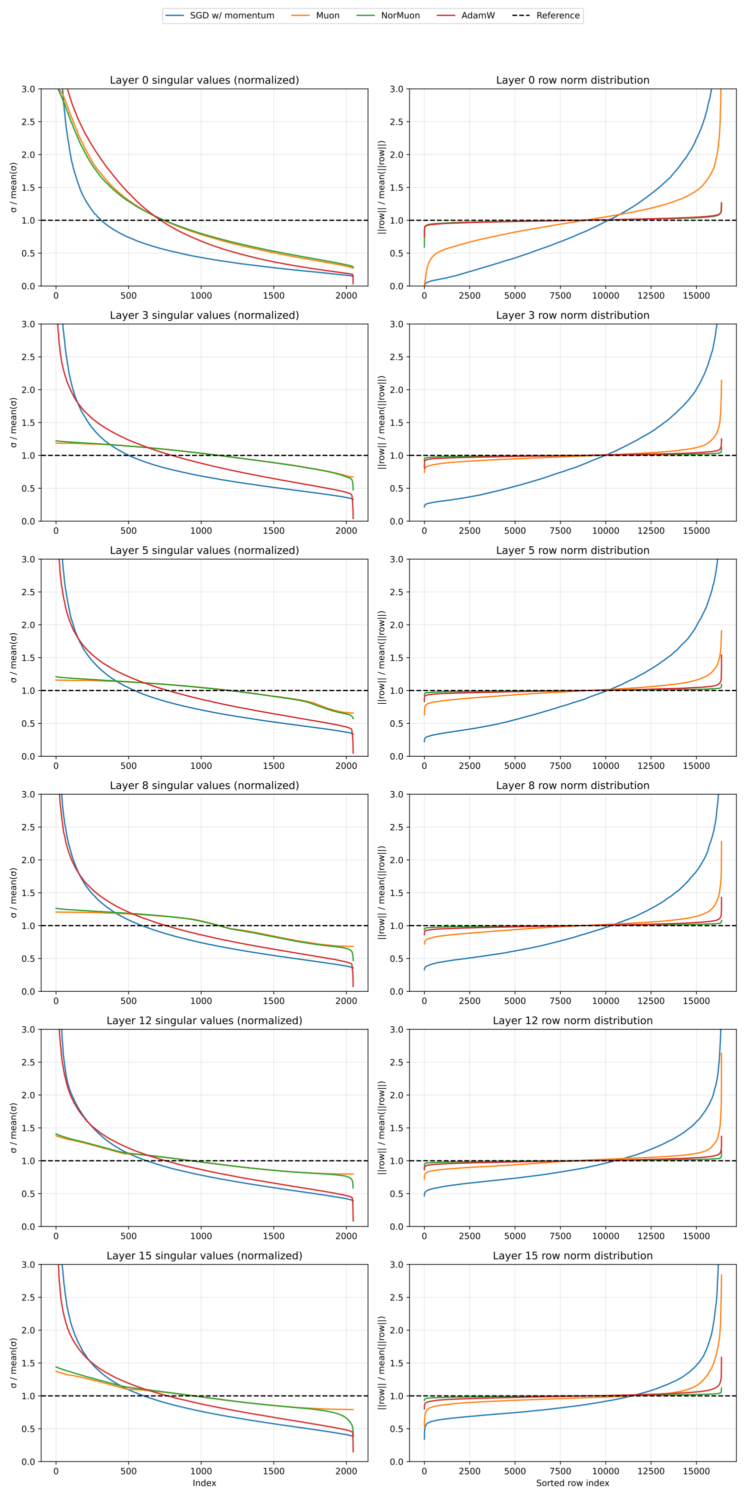

Figure 10: Visualization of optimization geometry on different layers on 1.1B model pretraining early checkpoints (10B).

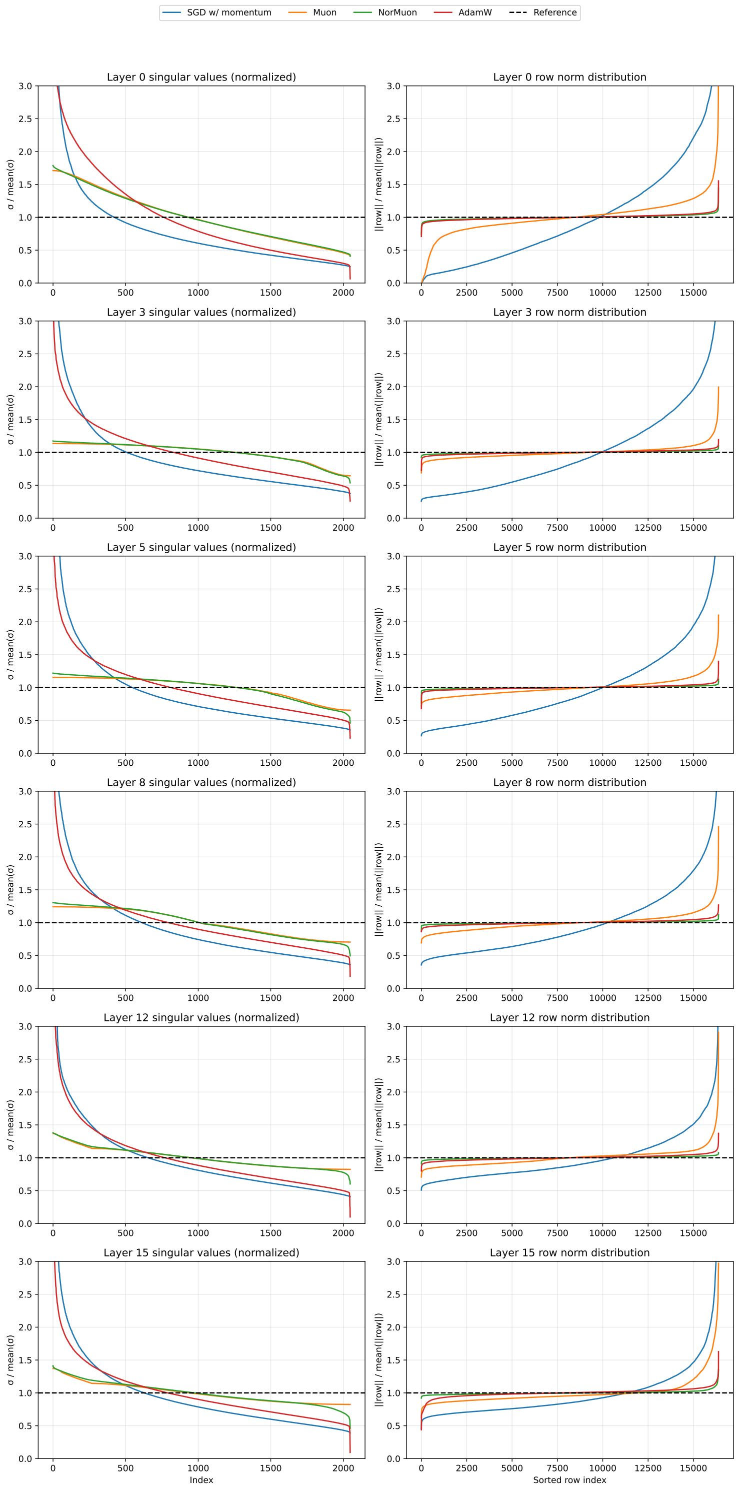

Figure 11: Visualization of optimization geometry on different layers on 1.1B model pretraining middle checkpoints (30B).

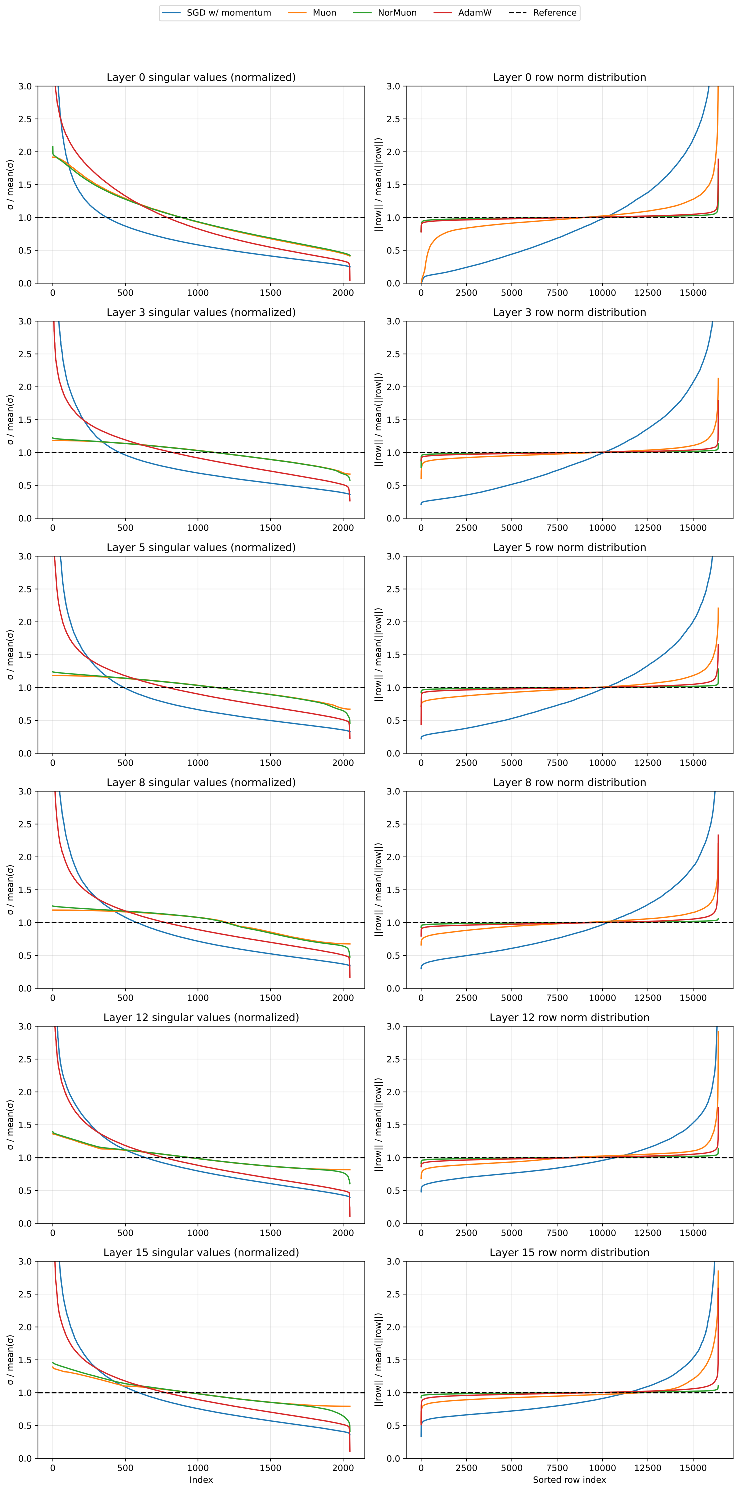

Figure 12: Visualization of optimization geometry on different layers on 1.1B model pretraining final checkpoints (50B).